Directional Superradiant Emission from Statistically Independent Incoherent Nonclassical and Classical Sources

S. Oppel,[1,2] R. Wiegner,[1] G. S. Agarwal,[2,3] and J. von Zanthier[1,2]
[1]*Institut für Optik, Information und Photonik, Universität Erlangen-Nürnberg, 91058 Erlangen, Germany*
[2]*Erlangen Graduate School in Advanced Optical Technologies (SAOT), Universität Erlangen-Nürnberg, 91052 Erlangen, Germany*
[3]*Department of Physics, Oklahoma State University, Stillwater, Oklahoma 74078, USA*

(Received 25 March 2014; published 30 December 2014)

Superradiance has been an outstanding problem in quantum optics since Dicke introduced the concept of enhanced directional spontaneous emission by an ensemble of identical two-level atoms. The effect is based on the correlated collective Dicke states which turn out to be highly entangled. Here we show that enhanced directional emission of spontaneous radiation can be produced also with statistically independent incoherent sources, via the measurement of higher-order correlation functions of the emitted radiation. Our analysis is applicable to a wide variety of quantum emitters, like trapped atoms, ions, quantum dots, or nitrogen-vacancy centers, and is also valid for incoherent classical emitters. This is experimentally confirmed with up to eight statistically independent thermal light sources. The arrangement to measure the higher-order correlation functions corresponds to a generalized Hanbury Brown–Twiss setup, demonstrating that the two phenomena, superradiance and the Hanbury Brown–Twiss effect, stem from the same interference phenomenon.

DOI: 10.1103/PhysRevLett.113.263606 PACS numbers: 42.50.Nn, 03.65.Ta, 03.67.Bg, 42.50.Dv

Dicke superradiance [1–5] remains an important problem in quantum optics primarily due to the inability to generate arbitrary symmetric Dicke states. Using single photons one can produce Dicke states where only one atom out of the ensemble is excited. For this case several groundbreaking experiments have been recently reported, including observation of collective Lamb shifts in regular arrays of nuclei [6,7] or directed forward scattering from atomic ensembles in collective first-excited [8–11] or Rydberg states [12–14]. However, the production of Dicke states with a higher number of excitations remains a challenge. One option is the repeated measurements of photons at particular positions starting from the fully excited system. This amounts to measuring the mth-order photon correlation function for $N > m$ emitters. In this case, if the detection is unable to identify the individual photon source, the collective system cascades down the ladder of symmetric Dicke states each time a photon is recorded via projective measurements. This is another example of measurement-induced entanglement among parties that do not directly interact with each other [15–22].

The inability to distinguish the emitters is fulfilled in the case of atoms confined to a region smaller than the wavelength λ of the emitted radiation. However, if the dipole-dipole interaction between the atoms is taken into account the collective system quickly leaves the symmetric subspace populating different super- and subradiant states, so the superradiant phenomena are obscured [3,5].

Indistinguishability of the emitters can also be ensured in case of widely separated sources as long as the detection occurs in the far field [1–5,23]. This is fulfilled, for example, for atomic clouds involving many particles, relevant for most experiments in the optical domain. However, in this regime the superradiant characteristics depend critically on the geometry of the sample due to diffraction and propagation effects [3,5], so the superradiant behavior is again obscured by geometrical considerations.

To study the effects of superradiance in an unobstructed manner the regime of a small number of widely spaced and motionless identical emitters appears most advantageous [23]. Despite recent progress [6,19,21,22,24–27] superradiant directional spontaneous emission has not been observed for this configuration.

In what follows we focus on superradiant emission in this regime by considering a small number of identical emitters localized at positions $\mathbf{R}_l$, $l = 1, \ldots, N$, along a linear chain with regular spacing $d \gg \lambda$ such that the dipole-dipole coupling between the emitters can be neglected (see Fig. 1). We start to investigate single-photon emitters (SPE), e.g., N two-level atoms with upper state $|e_l\rangle$ and ground state $|g_l\rangle$, $l = 1, \ldots, N$. We assume that the atomic chain is initially in the fully excited state $|S_N\rangle \equiv \prod_{l=1}^{N} |e_l\rangle$ and that $m < N$ photons spontaneously scattered by the atoms are recorded by m detectors located at positions $\mathbf{r}_j$, $j = 1, \ldots, m$, in the far field in a circle around the sources (see Fig. 1). For simplicity we suppose that the emitters and the detectors are in one plane and that the atomic dipole moments of the transition $|e_l\rangle \to |g_l\rangle$ are oriented perpendicular to this plane. The m-photon detection process can be described by the mth-order correlation function

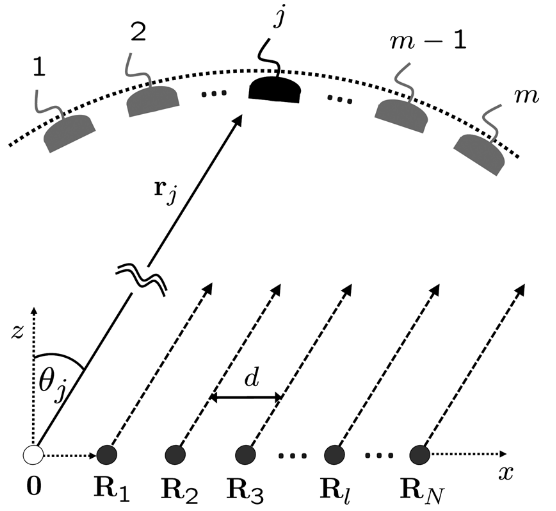

FIG. 1. Considered setup: N identical light sources, separated by a distance $d \gg \lambda$, are placed along a chain at positions $\mathbf{R}_l$, $l = 1, \ldots, N$; the light scattered by the sources is measured by m detectors, located at positions $\mathbf{r}_j$, $j = 1, \ldots, m$, in the far field.

$$G^{(m)}(\mathbf{r}_1, \ldots, \mathbf{r}_m) \equiv \left\langle : \prod_{j=1}^{m} \hat{E}^{(-)}(\mathbf{r}_j)\hat{E}^{(+)}(\mathbf{r}_j) : \right\rangle, \quad (1)$$

where $\langle : \ldots : \rangle$ denotes the normally ordered quantum mechanical expectation value. Because of the inability to identify the individual photon sources, the electric field operator at $\mathbf{r}_j$ is given by $[\hat{E}^{(-)}(\mathbf{r}_j)]^\dagger = \hat{E}^{(+)}(\mathbf{r}_j) \sim \sum_{l=1}^{N} e^{-i\varphi_{lj}} \hat{s}_l^-$ [18]. Here, $\hat{s}_l^- = |g_l\rangle\langle e_l|$ is the atomic lowering operator and $\varphi_{lj} = -k[(\mathbf{r}_j \cdot \mathbf{R}_l)/r_j] = -lkd \sin\theta_j$ denotes the optical phase accumulated by a photon emitted at $\mathbf{R}_l$ and detected at $\mathbf{r}_j$ relative to a photon emitted at the origin (see Fig. 1). Note that for simplicity we define the field and hence all correlation functions of mth order dimensionless; the actual values can be obtained by multiplying $G^{(m)}$ with m times the intensity of a single source.

Starting with all atoms in the state $|S_N\rangle$, we find from Eq. (1) for the mth-order correlation function, i.e., the angular distribution of the mth photon after $m - 1$ photons have been recorded [28],

$$G^{(m)}_{|S_N\rangle}(\theta_1, \ldots, \theta_m) \sim \left|\left| \sum_{\substack{\sigma_1,\ldots,\sigma_m=1 \\ \sigma_1 \neq \ldots \neq \sigma_m}}^{N} \prod_{j=1}^{m} e^{-i\varphi_{\sigma_j j}} |g_{\sigma_j}\rangle \right|\right|^2$$
$$= \sum_{\substack{\sigma_1,\ldots,\sigma_m=1 \\ \sigma_1 < \ldots < \sigma_m}}^{N} \left| \sum_{\substack{\sigma_1,\ldots,\sigma_m \\ \in \mathcal{S}_m}} \prod_{j=1}^{m} e^{-i\varphi_{\sigma_j j}} \right|^2. \quad (2)$$

Here, $|||\psi\rangle||^2 = \langle\psi|\psi\rangle$ defines the norm of the state vector $|\psi\rangle$, $|\ldots|$ abbreviate absolute values, and the expression $\sum_{\sigma_1,\ldots,\sigma_m \in \mathcal{S}_m}$ denotes the sum over the symmetric group $\mathcal{S}_m$ with elements $\sigma_1, \ldots, \sigma_m$. In Eq. (2) the products $\prod_{j=1}^{m} e^{-i\varphi_{\sigma_j j}}$ represent m-photon quantum paths where m photons emitted from m sources at $\mathbf{R}_{\sigma_j}$ and recorded by m detectors at $\mathbf{r}_j$ accumulate the phase $\sum_{j=1}^{m} \varphi_{\sigma_j j}$. Since the particular source of a recorded photon is unknown we have to sum over all possible combinations of m-photon quantum paths, which is expressed by the sum $\sum_{\sigma_1,\ldots,\sigma_m=1}^{N}$ in the first line of Eq. (2). Thereby the condition $\sigma_1 \neq \ldots \neq \sigma_m$ ensures that each detector records at most one photon. Considering that several combinations of m-photon quantum paths lead to the same final atomic state and thus have to be added coherently, we end up with the modulus square in the second line of Eq. (2). However, for the $\binom{N}{m}$ different final atomic states, the corresponding probabilities $|\ldots|^2$ have to be summed incoherently, which results in the first sum $\sum_{\sigma_1,\ldots,\sigma_m=1,\ \sigma_1<\ldots<\sigma_m}^{N}$ of the second line of Eq. (2).

We next consider that $m - 1$ detectors are placed at the same position θ_1 and the last detector at θ_2. Under this condition Eq. (2) takes the form [28]

$$G^{(m)}_{|S_N\rangle}(\theta_1, \ldots, \theta_1, \theta_2) \sim \frac{N-m}{N} + \frac{m-1}{N^2} \frac{\sin^2(N\frac{\varphi_{11}-\varphi_{12}}{2})}{\sin^2(\frac{\varphi_{11}-\varphi_{12}}{2})}. \quad (3)$$

Equation (3) as a function of θ_2 corresponds to the angular distribution of a photon spontaneously emitted by a system of N atoms in a symmetric Dicke state with $N - (m - 1)$ excitations [23]. It displays the corresponding superradiant emission characteristics: even though all N atoms emit spontaneously, the angular distribution of the probability to detect the mth photon at θ_2 equals the interference pattern of a coherently illuminated N slit grating, with the central maximum at $\theta_2 = \theta_1$. The distribution $G^{(m)}_{|S_N\rangle}(\theta_1, \ldots, \theta_1, \theta_2)$ for the initially uncorrelated state $|S_N\rangle$ as a function of θ_2 is thus identical to the mean radiated intensity of a symmetric Dicke state with $N - (m - 1)$ atoms in the excited state and $m - 1$ atoms in the ground state. The width $\delta\theta_2$ (FWHM) of the distribution $G^{(m)}_{|S_N\rangle}(\theta_1, \ldots, \theta_1, \theta_2)$ is given by

$$\delta\theta_2 \approx 2\pi/Nkd, \quad (4)$$

displaying an increasingly focused emission of the mth photon in the direction of θ_1 for growing numbers of emitters N. The visibility $\mathcal{V}_{\mathrm{SPE}} = (m - 1)/[m + 1 - (2m/N)]$ of the distribution vanishes for $m = 1$, illustrating the fact that the atoms emit incoherently, whereas for $m = N$ a maximum visibility of $\mathcal{V}_{\mathrm{SPE}} = 100\%$ is obtained. Figure 2 shows $G^{(m)}_{|S_N\rangle}(0, \ldots, 0, \theta_2)$ for $m = N$ as a function of θ_2 for $N = 2, 3, 5, 10$ SPE. Clearly, the width of the distribution decreases with increasing number of emitters N.

Note that the arrangement to measure $G^{(m)}_{|S_N\rangle}(\theta_1, \ldots, \theta_1, \theta_2)$ corresponds to a generalized Hanbury Brown–Twiss setup, where m detectors, located at positions $\mathbf{r}_j$, $j = 1, \ldots, m$, in the far field of the source coincidentally record m photons [29] (see Fig. 1). The superradiant

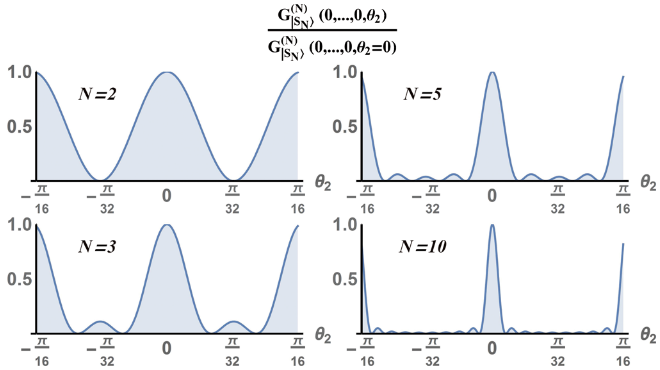

FIG. 2 (color online). Plot of the mth order correlation function $G^{(m)}_{|S_N\rangle}(0,\ldots,0,\theta_2)$ for $N = m = 2, 3, 5, 10$ single photon emitters (SPE) and $kd = 10\pi$. For a better comparison each function is normalized to its maximum value. To keep the focus to the central maximum we chose $\theta_2 \in [-\pi/16, +\pi/16]$.

spontaneous emission characteristics by a system of N atoms in a symmetric Dicke state with $N-(m-1)$ excitations is thus produced by a Hanbury Brown–Twiss intensity interferometer measuring $G^{(m)}_{|S_N\rangle}(\theta_1,\ldots,\theta_1,\theta_2)$. Thereby, the measurement of the first $m-1$ photons along θ_1 projects the uncorrelated initial state $|S_N\rangle$ into the symmetric Dicke state of excitation $N-(m-1)$ [18,28], leading to the subsequent superradiant emission of the mth photon.

The same focused emission pattern can also be observed with statistically independent incoherent classical sources. In this case each emitter may contribute not only a single photon to the mth-order correlation function, but up to m photons. This amounts to considering for the mth-order correlation function $G^{(m)}_N(\theta_1,\ldots,\theta_1,\theta_2)$ all possible combinations of m_l photons stemming from source l such that $\sum_{l=1}^N m_l = m$, or, in other words, all partitions of the number m, by keeping trace of the phase factors of the various m-photon quantum paths. The detailed calculation shows that each individual partition displays a focused spatial emission pattern of the same form as given by Eq. (3) [28]. Superposing all partitions—weighted with the corresponding statistics–thus leads, apart from an offset, to the same focused angular distribution as in case of N SPE. For example, for N statistically independent incoherent thermal light sources (TLS) with Gaussian statistics we obtain [28]

$$G^{(m)}_{\mathrm{NTLS}}(\theta_1,\ldots,\theta_1,\theta_2) \sim 1 + \frac{m-1}{N^2}\frac{\sin^2(N\frac{\varphi_{11}-\varphi_{12}}{2})}{\sin^2(\frac{\varphi_{11}-\varphi_{12}}{2})}, \quad (5)$$

displaying the same probability to detect the mth photon in the direction $\theta_2 = \theta_1$ after $m-1$ photons have been recorded at θ_1 as in case of N SPE.

The directional emission in case of light from thermal sources can again be understood in terms of quantum state projection. For N statistically independent TLS the density matrix reads $\rho_{\mathrm{NTLS}} = \prod_{l=1}^N \rho_l$, with $\rho_l = e^{-\hat{a}_l^\dagger \hat{a}_l/k_BT}/\mathrm{Tr}(e^{-\hat{a}_l^\dagger \hat{a}_l})$, where k_B is the Boltzmann constant and $\hat{a}_l$ the bosonic annihilation operator for the lth source. The detection of $m-1$ photons at θ_1 projects ρ_{NTLS} onto $\rho^{(m-1)}_{\mathrm{NTLS}} = (\sum_{l=1}^N e^{-i\varphi_{l1}}\hat{a}_l)^{m-1}\rho(\sum_{l=1}^N e^{-i\varphi_{l1}}\hat{a}_l^\dagger)^{m-1}$. In contrast to ρ_{NTLS} the density matrix $\rho^{(m-1)}_{\mathrm{NTLS}}$ displays nonvanishing correlations $\mathrm{Tr}[\hat{a}_i^\dagger \hat{a}_j \rho^{(m-1)}] \neq 0$, leading to a superradiant emission of the last photon in the same way as for Dicke states of excitation $N-(m-1)$ [see [4], Eq. (9.72)] or N projected statistically independent SPE [28]. The visibility $\mathcal{V}_{\mathrm{TLS}} = (m-1)/(m+1)$ of $G^{(m)}_{\mathrm{NTLS}}(\theta_1,\ldots,\theta_1,\theta_2)$ is slightly reduced with respect to $\mathcal{V}_{\mathrm{SPE}}$, vanishing again for $m=1$ since all sources emit incoherently, whereas for large m $\mathcal{V}_{\mathrm{TLS}}$ approaches 100%, independent of N. A similar result is obtained also with N statistically independent coherent light sources, displaying the same width $\delta\theta_2$ as in case of TLS or SPE [Eq. (4)] and an intermediate visibility $\mathcal{V}_{\mathrm{TLS}} < \mathcal{V}_{\mathrm{CLS}} < \mathcal{V}_{\mathrm{SPE}}$ [28]. Note that in case of classical light sources the correlation function does not vanish for $m > N$ since each light source may scatter more than one photon.

To measure $G^{(m)}_{\mathrm{NTLS}}(\theta_1,\ldots,\theta_1,\theta_2)$ for N statistically independent incoherent TLS we used a mask with N identical slits of width $a = 25\ \mu$m and separation $d = 200\ \mu$m, placed a few centimeters behind a rotating ground glass disk illuminated by a linearly polarized frequency-doubled Nd:YAG laser at $\lambda = 532$ nm (see Fig. 3). The large number of time-dependent speckles generated within each slit, produced by the stochastically interfering waves scattered from the granular surface of the ground glass disk, represent many independent pointlike subsources equivalent to an ordinary spatially incoherent thermal source. The coherence time of the pseudothermal sources depends on the rotational speed of the disk [30] and was chosen to $\tau_c \approx 50$ ms. The incident laser beam was enlarged to 1 cm to ensure a homogeneous illumination of the mask so that all N TLS radiate with equal intensity. Since multiphoton interferences of classical sources can be measured in the high-intensity regime [31] we used a conventional digital camera to determine $G^{(m)}_{\mathrm{NTLS}}(\theta_1,\ldots,\theta_m)$ placed in the focal point (Fourier plane) of a lens behind the mask ($z \approx f$), thus fulfilling the far field condition. Hereby,

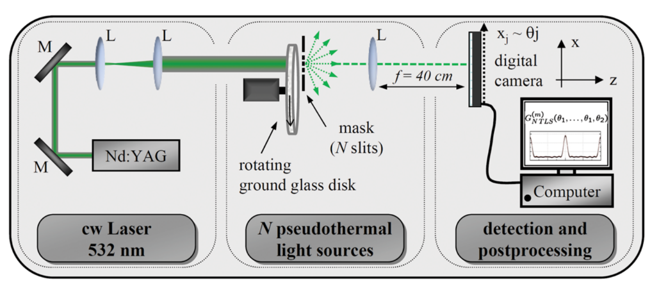

FIG. 3 (color online). Experimental setup to measure $G^{(m)}_{\mathrm{NTLS}}(\theta_1,\ldots,\theta_1,\theta_2)$ with N pseudothermal light sources. For details see text. M: mirror, L: lens.

each pixel of the camera may serve as a detector to register the intensity at position $x_j/z \sim \theta_j$. In order to evaluate $G^{(m)}_{\mathrm{NTLS}}(\theta_1, \ldots, \theta_1, \theta_2)$ we correlated $m-1$ pixels at $x_1 \sim \theta_1$, each separated by one pixel along the y direction to use $m-1$ different pixels with identical x_1 values, with another pixel at $x_2 \sim \theta_2$. With more than 1×10^6 pixels, a digital camera has the advantage that the amount of data accumulated in one frame to correlate the intensities at m different pixels is exceedingly higher than using m single-photon detectors [32]. In order to obtain interference signals of high visibility, the integration time of the camera τ_i was chosen to be much shorter than the coherence time of the TLS, in our case $\tau_i \approx 1$ ms $\ll \tau_c$.

Figure 4 displays the experimental results for $G^{(m)}_{\mathrm{NTLS}}(0, \ldots, 0, x_2)$ as a function of x_2 for $m = N = 2, \ldots, 8$. To verify the absence of first-order coherence the averaged intensity $I_{2\mathrm{TLS}}(x_2)$ in the case of 2 TLS was measured [see Fig. 4(a)]. As expected, the intensity is constant, confirming the spatial incoherence of the pseudothermal sources. The distribution $G^{(m)}_{\mathrm{NTLS}}(0, \ldots, 0, x_2)$ for different $m = N$ are shown in Figs. 4(b)–4(h). They are in excellent agreement with the theoretical predictions of Eq. (5). In particular, the increased probability to detect the Nth photon at $x_2 = 0$ after $N-1$ photons have been recorded at $x_1 = 0$ as a function of N is clearly visible.

The foregoing theoretical calculations and experimental results show that beyond entangled symmetric Dicke states it is also possible to employ initially uncorrelated incoherent light sources to obtain a focused spatial emission pattern of the emitted radiation. In case of initially uncorrelated SPE, e.g., N two-level atoms in the excited state, the directional spontaneous emission of the mth photon results from the preceding measurement of $m-1$ photons along selected directions, projecting the uncorrelated atoms onto Dicke states of excitation $N-(m-1)$ $(N \geq m > 1)$. The same behavior, i.e., an enhanced probability to detect the mth photon at θ_1 after $m-1$ photons have been recorded at θ_1, is obtained for statistically independent incoherent classical sources, due to projection of the initial state onto $\rho^{(m-1)}_{\mathrm{NTLS}}$ [28]. Note that the superradiant emission of the mth photon by initially uncorrelated incoherent light sources comes at the cost of reduced count rates due to the foregoing conditional measurement of $m-1$ photons at θ_1 (see, e.g., [18,33]). In a first approximation, if the probability to detect a single photon is $p = \eta\Delta\Omega/(4\pi)$, where η is the detection efficiency and $\Delta\Omega$ the solid angle subtended by each detector, the ratio of the conditional to the unconditional count rate is given by the ratio between the binomial distributions $P(N, p, k \geq m-1) := 1 - [\sum_{k=0}^{m-2} \binom{N}{k} p^k (1-p)^{N-k}]$ and $P(N, p, k \geq 1)$, where N is the total photon flux. Taking into account the particular geometry of the setup in Fig. 4 as well as the digital camera with its 10^6 detectors (pixels) and $\eta \approx 0.6$ we obtain $p = 2.7 \times 10^{-6}$, so that for a photon flux of $N = 3 \times 10^5$ s^{-1} we obtain for, e.g., $m = 8$ a ratio of 4.1×10^{-5}. For classical light sources where the photon flux can be much higher (in our case $N \approx 3 \times 10^{15}$ s^{-1}) this is not a serious drawback; for example, measuring $g^{(8)}_{\mathrm{NTLS}}(0, \ldots, 0, x_2)$ in Fig. 4 took a few minutes.

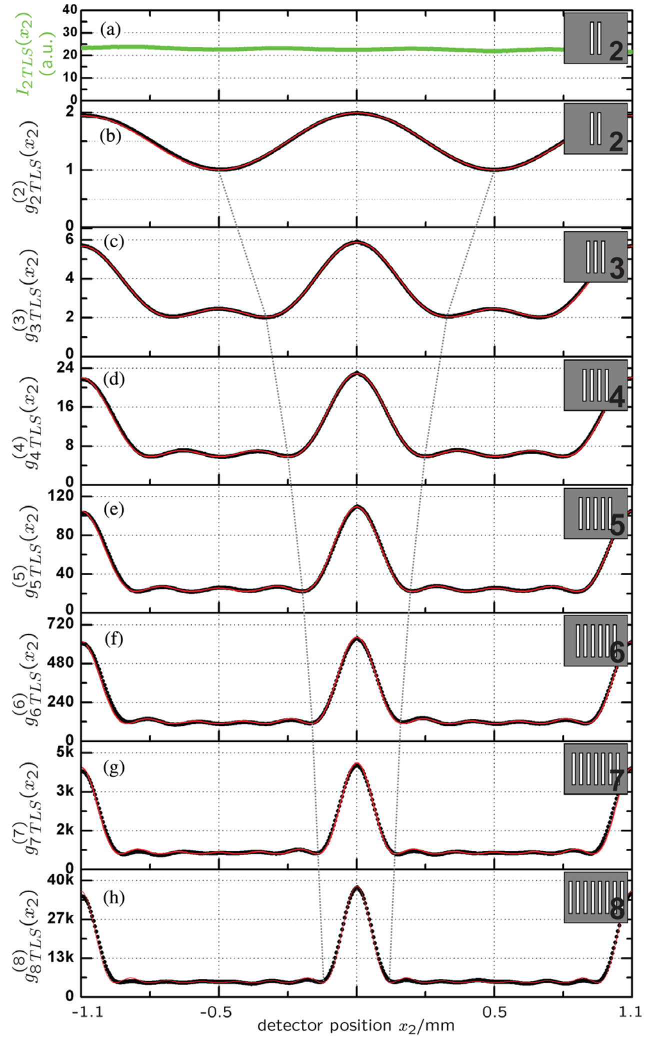

FIG. 4 (color online). Experimental results. (a) Average intensity $I_{2\mathrm{TLS}}(x_2)$ of 2 TLS demonstrating that the pseudothermal light sources are spatially incoherent in first order. (b)–(h) Measurement of the normalized mth-order correlation function $g^{(m)}_{\mathrm{NTLS}}(0,\ldots,0,x_2) = G^{(m)}_{\mathrm{NTLS}}(0,\ldots,0,x_2)/\{[I_{1\mathrm{TLS}}(0)]^{m-1} I_{1\mathrm{TLS}}(x_2)\}$ for $m = N = 2, \ldots, 8$ as a function of the mth detector at x_2. The focused emission of the mth photon at $x_2 = 0$ after $m-1$ photons have been recorded at $x_1 = 0$ is clearly visible. The theoretical prediction of Eq. (5) are displayed by the red (solid) curves. Fit parameters are an offset and a global prefactor.

We finally note that the superradiant emission characteristics of statistically independent incoherent light sources is obtained with a generalized Hanbury Brown–Twiss setup, demonstrating that the two phenomena, superradiance and the Hanbury Brown–Twiss effect, are two sides of the same coin.

The authors gratefully acknowledge funding by the Erlangen Graduate School in Advanced Optical Technologies (SAOT) by the German Research Foundation (DFG) in the framework of the German excellence initiative. R. W. and S. O. gratefully acknowledge financial support by the Elite Network of Bavaria and the hospitality of Oklahoma State University. This work was supported by DFG Research Grant No. ZA 293/4-1.

[1] R. H. Dicke, Phys. Rev. **93**, 99 (1954).
[2] N. E. Rehler and J. H. Eberly, Phys. Rev. A **3**, 1735 (1971).
[3] R. Friedberg, S. R. Hartmann, and J. T. Manassah, Phys. Rep. **7**, 101 (1973).
[4] G. S. Agarwal, *Quantum Optics*, Springer Tracts in Modern Physics, Vol. 70 (Springer, Berlin, Heidelberg, 1974).
[5] M. Gross and S. Haroche, Phys. Rep. **93**, 301 (1982).
[6] R. Röhlsberger, K. Schlage, B. Sahoo, S. Couet, and R. Rüffer, Science **328**, 1248 (2010).
[7] M. O. Scully and A. A. Svidzinsky, Science **328**, 1239 (2010).
[8] A. Kuzmich, W. P. Bowen, A. D. Boozer, A. Boca, C. W. Chou, L.-M. Duan, and H. J. Kimble, Nature (London) **423**, 731 (2003).
[9] C. H. van der Wal *et al.*, Science **301**, 196 (2003).
[10] C. W. Chou, S. V. Polyakov, A. Kuzmich, and H. J. Kimble, Phys. Rev. Lett. **92**, 213601 (2004).
[11] A. T. Black, J. K. Thompson, and V. Vuletić, Phys. Rev. Lett. **95**, 133601 (2005).
[12] Y. O. Dudin and A. Kuzmich, Science **336**, 887 (2012).
[13] T. Peyronel, O. Firstenberg, Q.-Y. Liang, S. Hofferberth, A. V. Gorshkov, T. Pohl, M. D. Lukin, and V. Vuletić, Nature (London) **488**, 57 (2012).
[14] D. Maxwell, D. Szwer, D. Paredes-Barato, H. Busche, J. Pritchard, A. Gauguet, K. Weatherill, M. Jones, and C. Adams, Phys. Rev. Lett. **110**, 103001 (2013).
[15] C. Cabrillo, J. I. Cirac, P. García-Fernández, and P. Zoller, Phys. Rev. A **59**, 1025 (1999).
[16] C. Skornia, J. von Zanthier, G. S. Agarwal, E. Werner, and H. Walther, Phys. Rev. A **64**, 063801 (2001).
[17] C. W. Chou, H. de Riedmatten, D. Felinto, S. V. Polyakov, S. J. van Enk, and H. J. Kimble, Nature (London) **438**, 828 (2005).
[18] C. Thiel, J. von Zanthier, T. Bastin, E. Solano, and G. S. Agarwal, Phys. Rev. Lett. **99**, 193602 (2007).
[19] D. L. Moehring, P. Maunz, S. Olmschenk, K. C. Younge, D. N. Matsukevich, L.-M. Duan, and C. Monroe, Nature (London) **449**, 68 (2007).
[20] K. S. Choi, A. Goban, S. B. Papp, S. J. van Enk, and H. J. Kimble, Nature (London) **468**, 412 (2010).
[21] J. Hofmann, M. Krug, N. Ortegel, L. Gerard, M. Weber, W. Rosenfeld, and H. Weinfurter, Science **337**, 72 (2012).
[22] H. Bernien *et al.*, Nature (London) **497**, 86 (2013).
[23] R. Wiegner, J. von Zanthier, and G. S. Agarwal, Phys. Rev. A **84**, 023805 (2011).
[24] R. G. DeVoe and R. G. Brewer, Phys. Rev. Lett. **76**, 2049 (1996).
[25] D. Leibfried *et al.*, Nature (London) **438**, 639 (2005).
[26] H. Häffner *et al.*, Nature (London) **438**, 643 (2005).
[27] T. Monz, P. Schindler, J. T. Barreiro, M. Chwalla, D. Nigg, W. A. Coish, M. Harlander, W. Hänsel, M. Hennrich, and R. Blatt, Phys. Rev. Lett. **106**, 130506 (2011).
[28] R. Wiegner, S. Oppel, D. Bhatti, J. von Zanthier, and G. S. Agarwal (to be published).
[29] R. Hanbury Brown and R. Q. Twiss, Nature (London) **177**, 27 (1956).
[30] L. E. Estes, L. M. Narducci, and R. A. Tuft, J. Opt. Soc. Am. **61**, 1301 (1971).
[31] I. N. Agafonov, M. V. Chekhova, T. Sh. Iskhakov, and A. N. Penin, Phys. Rev. A **77**, 053801 (2008).
[32] S. Oppel, T. Büttner, P. Kok, and J. von Zanthier, Phys. Rev. Lett. **109**, 233603 (2012).
[33] U. Schilling, C. Thiel, E. Solano, T. Bastin, and J. von Zanthier, Phys. Rev. A **80**, 022312 (2009).